

# Modeling of Immobilized Cell Columns for Bioconversion and Wastewater Treatment

Tingyue Gu\* and Mei-Jywan Syu†

Department of Chemical Engineering, Ohio University, Athens, Ohio 45701, and Department of Chemical Engineering, National Cheng Kung University, Tainan, Taiwan 70101



Immobilized cells are widely used in bioconversions to produce biological products as well as in wastewater treatment such as solvent removal from wastewater streams. In this work, a rate model is proposed to simulate this kind of process in an axial-flow fixed-bed column packed with porous particles containing immobilized cells. The transient model considered various mass transfer mechanisms including axial dispersion, interfacial film mass transfer, and intraparticle diffusion. Cell death in the immobilized cell system was also considered. Effects of various parameters such as kinetic constants and mass transfer parameters were studied. Operational situations such as feed fluctuation flow rate increase and two columns in series were also investigated. The model can be used to study the behavior and characteristics of immobilized cell columns in order to perform scale-up predictions of effluent profiles and for the purpose of process optimization.

## Introduction

Cell immobilization is an alternative to enzyme immobilization. It is almost as common as enzyme immobilization (1). It utilizes enzymes in living cells to carry out enzymatic reactions directly instead of purifying the enzyme molecules and subsequently immobilizing them onto a support, such as the stationary phase of a column. Immobilized cell systems can perform multistep, cofactor-requiring bioconversions that are not possible in immobilized enzyme systems (1). Scott (2) and Mosbach (3) have reviewed various cell immobilization methods. A more recent review on microencapsulation of microbial cells was given by Park and Chang (4). In a 2003 paper, Lozinsky et al. (5) commented on the use of polymeric cryogels for cell immobilization. Seki and Furusaki (6) developed a small immobilized cell system for taxol production. Immobilized cell systems are well-suited for waste treatment (7) such as decontamination of groundwater (8) because a continuous stream of liquid feed can be pumped into the column for an extended period of time. It does not have the cell washout problem that is common at high dilution rates for suspension reactors. Chen et al. (9) studied real-time control of an immobilized-cell reactor for wastewater treatment using oxidation–reduction potential. Cohen (10) reviewed biofiltration with immobilized cells for the treatment of fluids. Martin and Mengs (11) investigated the kinetics of degradation and viability of immobilized cells in a bioremediation system.

Enhanced productions can be achieved using immobilized-cell systems compared to suspension systems. Freeman and Lilly summarized various advantages of using immobilized cells (12). Kim et al. (13) achieved 14- to 23-fold higher kasugamycin productivity by immobilizing *Streptomyces kasugaensis* in a continuous bioreactor

compared to that in a suspension batch culture. Manohar et al. (14) obtained enhanced degradation of naphthalene by immobilization of a *Pseudomonas* strain in polyurethane foam. Tanaka et al. (15) edited a book on the industrial applications of immobilized enzymes and cells.

Various models have been proposed for immobilized-cell packed bed reactors. However, so far there is no transient model that simultaneously considers all three mass transfer mechanisms, i.e., axial dispersion, interfacial film mass transfer, and intraparticle diffusion. Most studies emphasized diffusion in polymer matrix or particle macropores (16–20). Langley et al. (8) studied intraparticle diffusion in spherical immobilized cell particles for denitrification at steady state. Wu et al. (19) considered axial dispersion in a tube packed with immobilized cells. Nath and Chand (20) studied interfacial film mass transfer coupled with a pseudo-first-order reaction for bioconversion of sugars to ethanol using immobilized yeast cells. Zheng and Gu (21) investigated the startup period of a bioreactor column with immobilized *Lactobacillus delbrueckii* by using a theoretical solution to a model that considered axial dispersion and linear reaction kinetics. It is well-known that immobilized-cell systems, like immobilized enzyme systems, suffer from mass transfer resistances (1). In this work, axial dispersion, interfacial film mass transfer between the bulk-fluid phase and the particle surfaces, and intraparticle diffusion were all considered as well as cell death for a fix-bed column with immobilized cells. Nonlinear Monod kinetics was used. The model was solved numerically.

**Mathematical Model.** The following assumptions are needed: (1) substrate conversion is carried out by working immobilized cells only, (2) dislodged cells in the particle macropores and bed void space are considered dead or nonfunctional and can be ignored, (3) immobilized cell mass concentration is uniform along the column length and may be a function of time, and (4) particles are considered uniform spheres. On the basis of these

\* To whom correspondence should be addressed. Tel: 740-593-1499. Fax 740-593-0873. E-mail address: gu@ohio.edu.

† National Cheng Kung University.

assumptions, the following equation can be written based on differential mass balances.

(1) Bulk-fluid phase governing equation:

$$-D_{bi} \frac{\partial^2 C_{bi}}{\partial Z^2} + v \frac{\partial C_{bi}}{\partial Z} + \frac{\partial C_{bi}}{\partial t} + \frac{3k_f(1 - \epsilon_b)}{\epsilon_b R_p} (C_{bi} - C_{p,i,R=R_p}) = 0 \quad (1)$$

(2) Particle phase governing equation:

$$\epsilon_p \frac{\partial C_{pi}}{\partial t} - R_{ai} - \epsilon_p D_{pi} \left[ \frac{1}{R^2} \frac{\partial}{\partial R} \left( R^2 \frac{\partial C_{pi}}{\partial R} \right) \right] = 0 \quad (2)$$

where  $D_{pi}$  is the diffusivity of component  $i$  inside particle macropores. Particle porosity is not lumped into  $D_{pi}$  in this work. Substrate is denoted as component 1 ( $i = 1$ ) and product component 2 ( $i = 2$ ).  $R_{ai}$  is the rate of addition of substrate or product per unit volume of particle including macropores and particle skeleton. Equation 2 can be obtained from a shell mass balance on a spherical shell containing macropores and the solid skeleton inside a particle. It should be pointed out that the  $R_{ai}$  term must be multiplied by  $(1 - \epsilon_p)$  in eq 2 if  $R_{ai}$  is based on the unit volume of particle skeleton. Not surprisingly, eq 1 is identical to that used in liquid chromatography modeling (22) because no reaction is considered in the bulk-fluid phase. The following initial and boundary conditions are needed for the model:

Initial conditions:

$$\text{at } t = 0, C_{bi} = C_{bi}(0, Z), C_{pi} = C_{pi}(0, R, Z)$$

Boundary conditions:

$$\text{at } Z = 0, \partial C_{bi} / \partial Z = v(C_{bi} - C_{fi}(t)) / D_{bi}; \text{ and at } Z = 1, \partial C_{bi} / \partial Z = 0$$

$$\text{at } R = 0, \partial C_{pi} / \partial R = 0; \text{ and at } R = 1, \partial C_{pi} / \partial R = k_f (C_{bi} - C_{p,i,r=1}) / (\epsilon_p D_{pi})$$

Define the following dimensionless parameters for nondimensionalization:

$$c_{bi} = C_{bi} / C_{0i}, c_{pi} = C_{pi} / C_{0i}, r = R / R_p, z = Z / L, Pe_{Li} = vL / D_{bi}, Bi_i = k_f R_p / (\epsilon_p D_{pi}), \eta_i = \epsilon_p D_{pi} L / (R_p^2 v), \xi_i = 3Bi_i \eta_i (1 - \epsilon_b) / \epsilon_b, \tau = vt / L, r_{ai} = R_{ai} L / (v C_{0i})$$

Because the product concentrations in the bulk-fluid phase and the particle phase are unknown beforehand, it can take an arbitrary value or the substrate feed concentration  $C_{01}$  for their nondimensionalization. After a simulation run is done, a more suitable value can be used to attenuate the output values. Equations 1 and 2 can be rewritten in dimensionless form as follows:

$$- \frac{1}{Pe_{Li}} \frac{\partial^2 c_{bi}}{\partial z^2} + \frac{\partial c_{bi}}{\partial z} + \frac{\partial c_{bi}}{\partial \tau} + \xi_i (c_{bi} - c_{p,i,r=1}) = 0 \quad (3)$$

$$\epsilon_p \frac{\partial c_{pi}}{\partial \tau} - r_{ai} - \eta_i \left[ \frac{1}{r^2} \frac{\partial}{\partial r} \left( r^2 \frac{\partial c_{pi}}{\partial r} \right) \right] = 0 \quad (4)$$

The dimensionless initial and boundary conditions are as follows:

Initial conditions:

$$\text{at } \tau = 0, c_{bi} = c_{bi}(0, z), c_{pi} = c_{pi}(0, r, z)$$

Boundary conditions:

$$\text{at } z = 0, \partial c_{bi} / \partial z = Pe_{Li} [c_{bi} - C_{fi}(\tau) / C_{0i}]; \text{ and at } z = 1, \partial c_{bi} / \partial z = 0$$

at  $r = 0, \partial c_{pi} / \partial r = 0$ ; and at

$$r = 1, \partial c_{pi} / \partial r = Bi_i (c_{bi} - c_{p,i,r=1})$$

$C_{fi}(\tau) / C_{0i}$  is the dimensionless feed concentration profile of component  $i$ . It is a function of dimensionless time  $\tau$ .

If Monod kinetics is assumed, the following equation can be written:

$$-R_{a1} = k_s S X / (K_s + S) \quad (5)$$

where  $k_s$  is the maximum specific substrate utilization rate averaged over the entire particle volume ( $L, \theta$ ) and  $S$  is the substrate concentration in particle macropores that is designated as  $C_{p1}$  in the model. Only one substrate is considered. The negative sign in the equation above indicates that the substrate is consumed as time progresses. The following relationship exists for product formation (23):

$$R_{a2} = -Y_{P/S} R_{a1} \quad (6)$$

The effluent concentration of the product (component 2 in the model) is relatively unimportant since in many cases, such as in wastewater treatment, only substrate conversion is of concern. In this work, yield coefficient  $Y_{P/S}$  was assumed to be a constant. It was set to unity for convenience in mass balance checking.

For the substrate concentration in the particle phase, eq 5 gives

$$-r_{a1} = - \frac{R_{a1} L}{v C_{01}} = \frac{k_s c_{p1} X}{K_s + C_{p1}} \cdot \frac{L}{v} = \frac{Da_s c_{p1}}{(K_s / C_{01} + c_{p1})} \cdot \frac{X}{C_{01}} \quad (7)$$

in which  $Da_s = k_s L / v$  is defined as the dimensionless Damköhler number for substrate conversion. In the particle phase, the dimensionless substrate concentration is  $c_{p1}$ . For the product concentration in the particle phase, eq 6 leads to

$$r_{a2} = \frac{R_{a2} L}{v C_{02}} = \frac{-Y_{x/s} R_{a1} L}{v C_{02}} = -Y_{x/s} r_{a1} \cdot \frac{C_{01}}{C_{02}} \quad (8)$$

In wastewater treatment such as solvent removal from the wastewater streams produced by the electronics industry, the substrate concentration (e.g., acetone in the wastewater stream) in the effluent is the most important concern while the product concentration sometimes draws no attention at all.

Langley et al. (8) assumed a constant amount of immobilized cell mass along the bioreactor's length in their modeling of immobilized-cell denitrification. This is practical if the time frame for modeling is relatively small. Wu et al. (19) reported that immobilized cell mass decreased as particle aged in an immobilized-cell denitrification system. It was assumed in this work that the

immobilized cell mass concentration inside the particles declines exponentially with time as shown below:

$$\frac{X}{X_0} = \exp(-\lambda t) = \exp(-\tau\lambda L/v) \quad (9)$$

If a negative value is assigned to the death rate  $\lambda$ , eq 9 will describe exponential growth instead.

Equation 7 can be rewritten as follows:

$$-r_{a1} = \frac{c_{p1}}{(K_s/C_{01} + c_{p1})} \cdot \frac{(Da_s X_0)}{C_{01}} \cdot \exp(-\tau\lambda L/v) \quad (10)$$

in which  $Da_s X_0/C_{01}$  can be considered a combined dimensionless parameter. In eq 11, if there is no cell death, i.e.,  $\lambda = 0$ ,  $\exp(-\tau\lambda L/v)$  becomes unity.

Because eq 10 is nonlinear with respect to  $c_{p1}$ , the rate model system above can only be solved numerically. The finite element method was used for the discretization of  $z$  in eq 3, and the orthogonal collocation method for  $r$  in eq 4. Ten to sixteen quadratic finite elements and two interior collocation points were found to be adequate for all cases simulated in this work. The resultant ODE (ordinary differential equation) system was solved using a public domain ODE solver called VODE by Brown et al. (24). Simulated effluent profiles were plotted using  $q_b(\tau, 1)$  vs  $\tau$  data. A Fortran program was written and compiled for Microsoft Windows 98. It was run on a Pentium II personal computer. A typical simulation calculation in this work takes only a couple of seconds. For high-end personal computers, real-time simulation can be readily achieved.

## Results and Discussion

**Breakthrough Curves and Mass Balance of Concentration Profiles.** Figure 1 shows the breakthrough curves for a substrate feed concentration of 10 g/L. Parameters used for calculating Figure 1 are listed in Table 1. In the absence of cell death, Figure 1 shows that both the substrate concentration and the product concentration level off to a steady state. The effluent substrate concentration is 13.4% of the feed concentration, indicating a conversion rate of 86.6%.

In Figure 1, a dimensionless time of unity is equivalent to the time needed to elute out an effluent volume equaling to the bed void fraction multiplied by the column volume. It is the same as the blue dextrin retention time in pulse analysis (equivalent to the breakthrough time in breakthrough analysis) because blue dextrin does not penetrate particle macropores because of its large molecular size. In breakthrough analysis for liquid chromatography, the area above the dimensionless concentration and below the unity line is the so-called column hold-up capacity area that can be derived from the mass balance (22). For Figure 1, the column holdup capacity for the sum of substrate and product concentrations is equal to the area calculated from dimensionless time vs sum of substrate and product concentrations curve because  $Y_{P/S} = 1$ . The area integrated from the sum of substrate and product effluent profiles shown in Figure 1 is 1.611. It is the same as the value calculated from the formula for the column hold-up capacity area without any component binding to the particles (22):

$$A = (1/\epsilon_b - 1)\epsilon_p + 1 \quad (11)$$

This agreement is a partial validation of the software used in this work.

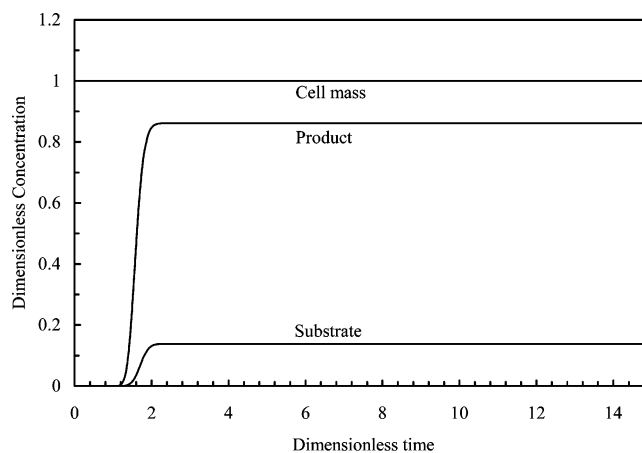


**Figure 1.** Simulated effluent substrate and product concentrations and cell mass concentration inside a column.

**Table 1. Parameter Values Used to Obtain Figure 1**

parameters	substrate ( $i = 1$ )	product ( $i = 2$ )
$Pe_{Li}$	500	500
$\eta_i$	5	5
$Bi_i$	3	3
$C_{0i}$ (g·L <sup>-1</sup> )	10	10
$K_s/C_{01}$		0.1
$Y_{P/S}$ (g·g <sup>-1</sup> )		1
$Da_s X_0/C_{01}$		$0.4 \times 2.2$
$\lambda L/v$		0
$\epsilon_p$		0.5
$\epsilon_b$		0.45

**Effect of Cell Death.** In wastewater treatment, the feed stream may not provide all of the nutrients needed by the cells for growth or for maintenance. Cell death will occur. It is important to monitor immobilized cell mass concentration  $X$ . When  $X$  becomes too low, a nutritious feed stream can be switched on to allow the cells to regain their population. Figure 2 shows the effect of cell death with a dimensionless death rate ( $\lambda L/v$ ) of 0.005 corresponding to a dimensionless half-life time of 138.6. This means that  $X$  will decrease by half after a time that is equivalent to 138.6 times the blue dextrin retention time on the column. The substrate and product effluent concentrations and the cell mass concentration inside the column with cell death are compared to those in Figure 1. Note that in Figure 2, the cell mass curve with cell death declines almost linearly. During the normal operational period of an immobilized-cell column, the change in  $X$  is quite slow. Within a limited time frame for a small  $\lambda L/v$  value,  $X/X_0$  changes almost linearly with time, as indicated by the following Taylor series expansion of an exponential function:

$$\exp(y) = 1 + y + y^2/2! + y^3/3! + \dots \quad (12)$$

When cell death occurs, there is no steady state in effluent profiles. The effluent substrate concentration continues to rise while the effluent product concentration and cell mass concentration inside the column decline. To simplify discussions on the effects of different parameters below, cell death was ignored.

**Effect of Substrate Feed Concentration and Its Fluctuation.** The substrate feed concentration for an immobilized-cell column may fluctuate. For example, the feed concentration of a primary toxic compound in a wastewater treatment process can vary. To simulate this effect, a feed profile with three steps is used for Figure 3. The parameters used in Figure 3 are the same as those

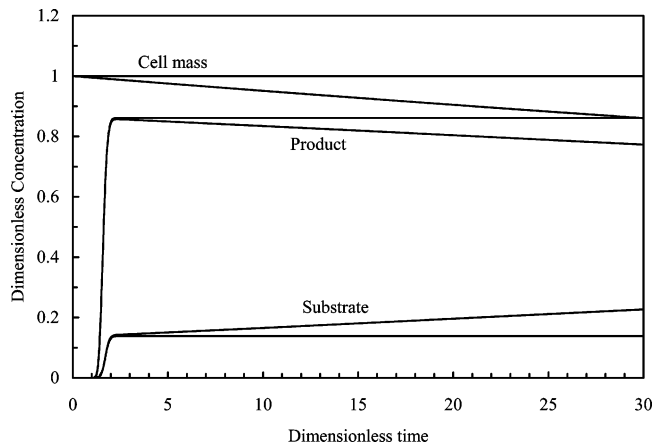


**Figure 2.** Effect of cell death.

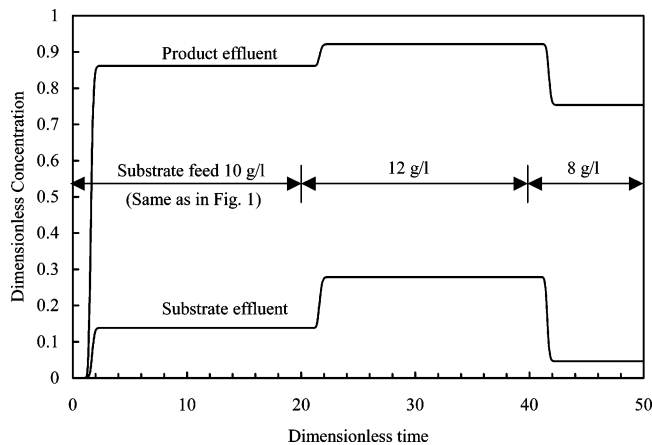


**Figure 3.** Effect of substrate feed concentration and its fluctuation.

in Figure 1 except for the feed profile. The dimensionless substrate feed concentrations based on the initial feed concentration of 10 g/L in the dimensionless time frame  $\tau \in [0,20)$ ,  $\tau \in [20,40)$ , and  $\tau \in [40,50]$  are 1.0, 1.2, and 0.8, respectively. As a result of the mass balance relationship between the substrate and the product with  $Y_{P/S} = 1$ , the sums of substrate concentration and product concentration in the three steady-state (flat) regions in Figure 3 are also easily shown to be 1.0, 1.2, and 0.8, respectively. Figure 3 shows that there is a delay in the response of effluent profiles after a step change in the feed.

Figure 3 also explains the effect of different substrate feed concentrations on the substrate conversion. It clearly shows that as the feed concentration increases, the substrate conversion rate is decreased, and vice versa. This is quite reasonable because the immobilized cells inside the column are overwhelmed when there is too much substrate in the feed.

**Effects of Initial Immobilized Cell Mass Concentration and Maximum Specific Substrate Utilization Rate.**  $X_0$  and  $k_s$  show up in the model system as a product ( $k_s X_0$ ) in  $Da_s X_0 / C_{01}$  in eq 10. Thus, the effects of  $X_0$  and  $k_s$  are the same. This means that the increase of  $k_s$  is equivalent to an increase of  $X_0$ , or the decrease of  $k_s$  can be offset by an increase in  $X_0$ . In Figure 4, the curves marked with  $-10\%$  and  $+10\%$  are results from changing  $X_0$  (or  $k_s$ ) by  $10\%$ . Figure 4 shows that a larger  $X_0$  (or  $k_s$ ) enhances substrate conversion.

**Effect of Monod Half-Velocity Constant.** The Monod half-velocity constant ( $K_s$ ) has a direct impact on

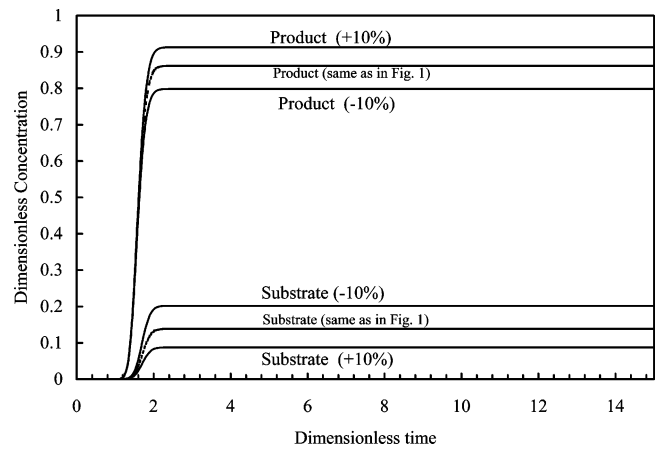


**Figure 4.** Effect of  $X_0$  and  $k_s$ .

substrate utilization according to eq 5. Figure 5 shows that its effect on effluent substrate and product profiles when its value increases or decreases by  $50\%$ . Figure 5 shows that a larger  $K_s$  inhibits substrate conversion. It is obvious that if the substrate feed concentration is low, the  $K_s$  effect will be more pronounced and vice versa according to eq 5.

**Effects of the Three Dimensionless Mass Transfer Parameters.** The effect of the Peclet number is shown in Figure 6. It was obtained on the basis of the parameters used for Figure 1 except with varied Peclet numbers of the substrate and product. It shows that a larger Peclet number will cause the breakthrough curve in the startup period to be stiffer (deliberately exaggerated by using a shorter  $x$ -axis scale in Figure 6), whereas the change on the substrate conversion rate is hardly noticeable. This means that the effect of axial dispersion on the steady-state substrate conversion rate is negligible for the parameters used in Figure 6. Figure 6 also shows that the effect of Peclet number on the startup period tapers off when its value becomes large.

The effect of Biot number is shown in Figure 7. Its effect is very similar to that of Peclet number. Figure 7 shows that increasing the Biot number beyond 30 produces almost no noticeable changes in effluent profiles. When its value is relatively large (i.e., relatively fast film mass transfer), the Biot number does not affect the substrate conversion rate significantly. However, if the film mass transfer coefficient is unusually small, which leads to an uncommonly small Biot number, indicating that film mass transfer is rate-limiting rather than intraparticle diffusion, the bioconversion of the substrate will be hampered considerably as seen by the  $Bi = 0.5$  curves in Figure 7. This is because some substrate in the bulk-fluid phase is swept away before it has a chance to enter the particle phase for bioconversion.

The effect of  $\eta$  number is shown in Figure 8. Increasing it will give sharper breakthrough curves and a better substrate conversion rate. Figure 8 also shows that increasing it beyond a value of 20 produces almost no further changes. As a matter of fact, all three dimensionless mass transfer parameters discussed above show this type of "saturation" behavior.

**Effect of Increased Column length.**  $Da_s$ ,  $Pe_{L,i}$ , and  $\eta_i$  values are directly proportional to column length. Based on Figure 1 parameters, Figure 9 was obtained by varying the  $Da_s$ ,  $Pe_{L,i}$ , and  $\eta_i$  values accordingly. It shows that increasing column length will improve bioconversion of the substrate.

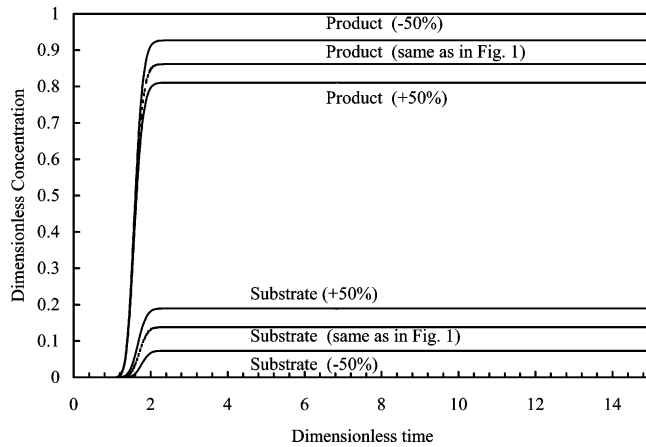


Figure 5. Effect of  $K_s$ .

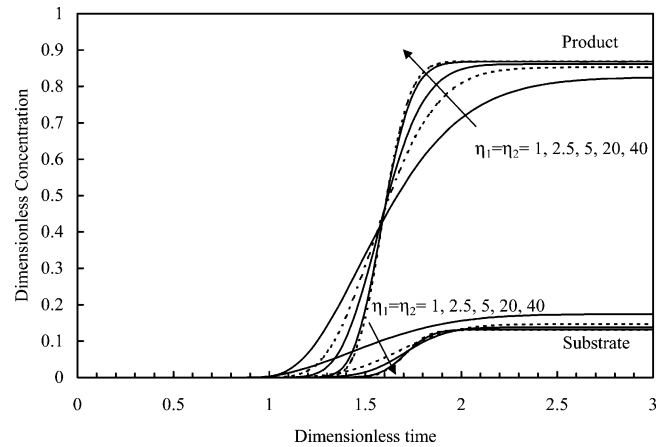


Figure 8. Effect of dimensionless mass transfer parameter  $\eta$ .

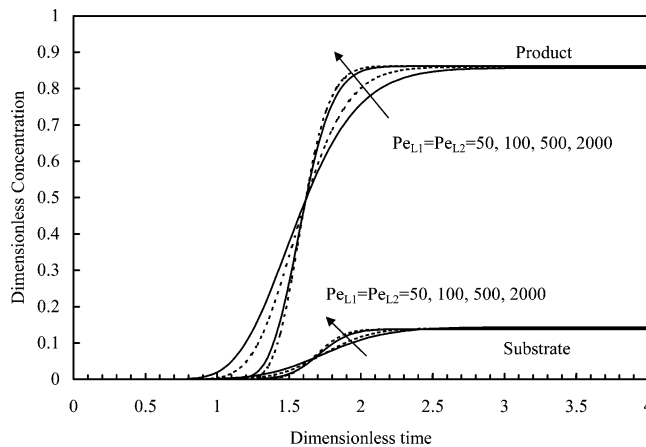


Figure 6. Effect of Peclet number.

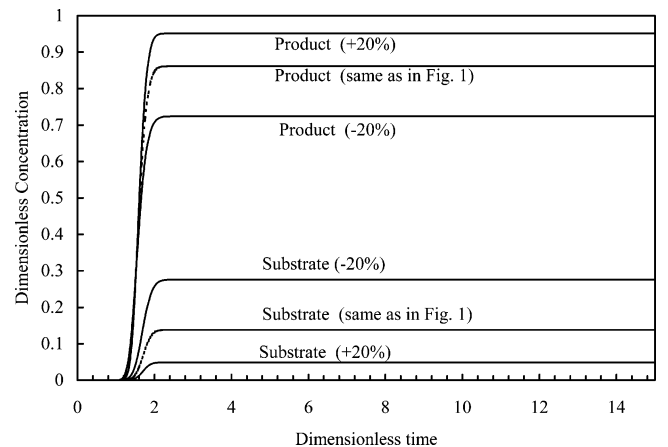


Figure 9. Effect of column length.

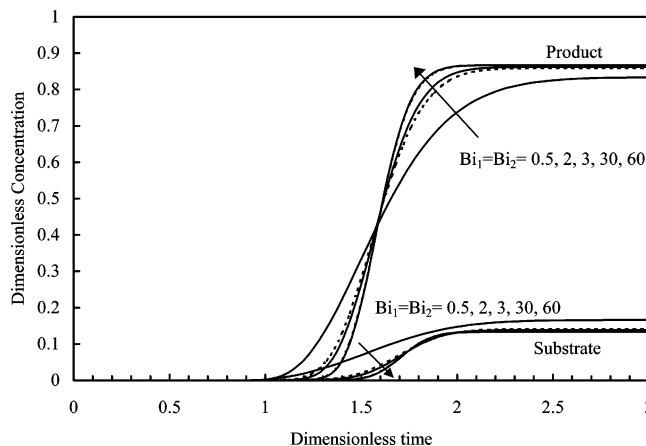


Figure 7. Effect of Biot number for mass transfer.

**Effect of Volumetric Flow Rate  $Q$ .** It is expected that increasing the volumetric flow rate will lower the substrate conversion rate. Volumetric flow rate is directly proportional to interstitial velocity:

$$v = \frac{4Q}{\pi d_c^2 \epsilon_b} \quad (13)$$

Changing  $v$  will cause axial dispersion coefficient  $D_{b,i}$  and interfacial film mass transfer coefficient  $k_i$  to vary. In a column packed with porous media, it is reasonable to use  $D_{b,i} \propto v$  (25, 26). On the basis of its definition, the Peclet number will not be affected by this relationship. Accord-

ing to the two experimental correlations by Pfeffer and Happel (27), it is reasonable to use (26)

$$k_i \propto v^{1/3} \quad (14)$$

This leads to

$$Bi_i \propto v^{1/3} \quad (15)$$

Equation 15 shows that doubling  $v$  will cause the Biot number to increase by 26.0%. On the basis of their definitions, it is obvious that  $Da_s$  and  $\eta_i$  are inversely proportional to  $Q$  or  $v$ . Doubling  $Q$  will greatly reduce the substrate conversion rate as shown in Figure 10. Figure 10 has the same parameters as in Figure 1 except that  $Da_s$ ,  $\eta_i$ , and  $Bi_i$  were changed by multiplying by 0.5, 0.5, and 1.26, respectively.

**Two Columns in Series.** It is necessary sometimes to use more than one column in series as a result of insufficient conversion of the substrate in one column. Because the software developed in this work for a single column can take a user-supplied data file with individual feed data points, it is easy to simulate multiple-column operations one at a time. In Figure 11, the first column output profiles were obtained using the same parameters as in Figure 1 except that the  $Da_s X_0 / C_{01}$  value was halved. Both the substrate and the product effluent profiles obtained from simulating the first column were then used as input data (to replace the previous steady substrate input) to obtain the effluent profiles for the second column as shown in Figure 11. Figure 11 clearly shows that the bioconversion of substrate was greatly improved

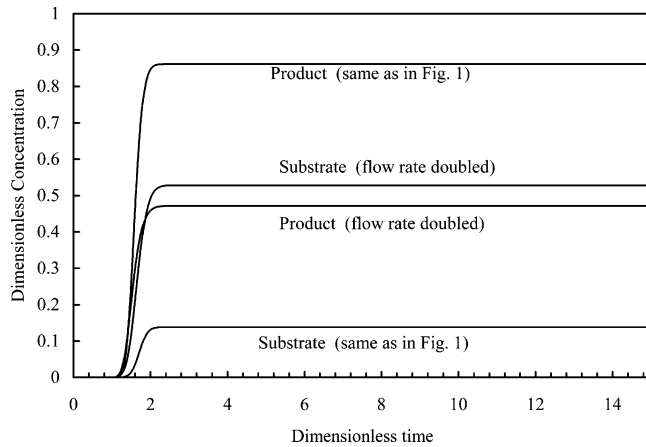


**Figure 10.** Effect of volumetric flow rate.

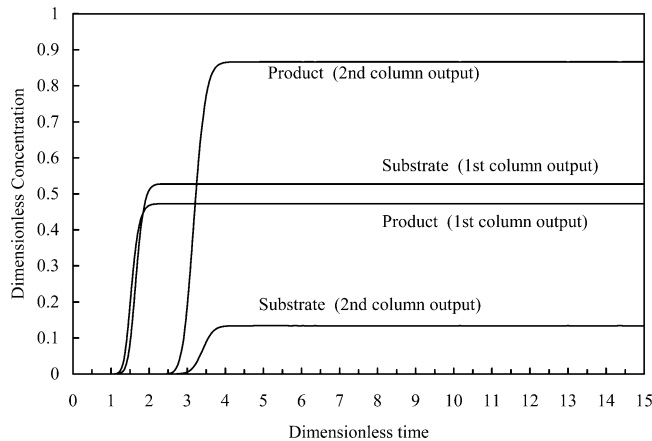


**Figure 11.** Two columns in series.

with the use of the second column. The final dimensionless substrate concentration in Figure 11 is 0.134, slightly better than 0.138 in Figure 1 that has a  $Da_s X_0 / C_{01}$  value twice as large (meaning  $k_s$  or  $X_0$  is twice as large). Using multiple columns in series gives operators more flexibility than using a long column. An additional column can be added on if feed overload occurs.

Effluent recycling can be simulated similar to simulating two columns in series. If the substrate conversion rate is not high enough at steady state, the fresh feed can be switched off. Lacking another column, the output stream can be collected and fed back to the same column. The effluent profiles from the first simulation run can be used to form the feed data directly for another run if the effluent stream of the column is kept in a tube loop without mixing before recycling. The effluent profiles can also be integrated before forming the feed data for another run if the recycle stream consists of a well-mixed solution of the first effluent stream. At the start of the feed recycle, if the column contains the leftover of the steady-state substrate and product concentrations, the initial values for the concentrations must be reset accordingly. This can be readily carried out in the Fortran software.

**Two Substrates in the Feed Stream.** If there are two substrates in the feed stream to be converted, the software can be run for one substrate at a time separately as long as the existence of one substrate does not interfere with the bioconversion of the other substrate. If interference does occur, the model system and software must be modified.

## Conclusions

This work presented a model for the simulation of immobilized-cell columns used in bioconversion or wastewater treatment. Axial dispersion, interfacial mass transfer, and intraparticle diffusion were all considered. Cell death was also included in the model. This model system should be adequate in describing mass transfer in a column packed with immobilized cell particles. It can simulate both the transient start-up period and the steady-state (in absence of cell death) effluent profiles. Effects of various parameters as well as different operational strategies in the model were investigated.

Different systems may have different bioconversions going on. The model system can be easily modified to account for different rate equations. If the rate equations are algebraic equations, their implementation in the Fortran code is straightforward because they are expressed in the Fortran code as formulas and they do not need discretization. The numerical treatment of the difficult mass transfer parts are unaffected. If a rate equation takes a first-order ODE form, the Fortran code needs to be modified by bundling the ODE with other ODEs. The Windows executable software used in this work can be obtained from the corresponding author free of charge for academic researchers.

## Acknowledgment

Authors wish to thank Taiwan's National Science Council for financial support.

## Notation

$Bi_i$	Biot number for mass-transfer of component $i$
$C_{0i}$	feed concentration of component $i$ used for non-dimensionalization ( $\text{g}\cdot\text{L}^{-1}$ )
$C_{bi}$	concentration of substrate ( $i = 1$ ) or product ( $i = 2$ ) in the bulk-fluid phase of the column ( $\text{g}\cdot\text{L}^{-1}$ )
$C_{fi}$	feed concentration profile of component $i$ ( $\text{g}\cdot\text{L}^{-1}$ )
$C_{pi}$	concentration of component $i$ in the stagnant fluid phase inside particle macropores ( $\text{g}\cdot\text{L}^{-1}$ )
$c_{bi}$	$= C_{bi} / C_{0i}$
$c_{pi}$	$= C_{pi} / C_{0i}$
$D_{bi}$	axial dispersion coefficient of component $i$ ( $\text{m}^2\cdot\text{s}^{-1}$ )
$D_{pi}$	effective diffusivity of component $i$ in particle macropores ( $\text{m}^2\cdot\text{s}^{-1}$ )
$Da_s$	$= k_s L / v$ , Damköhler number for substrate conversion
$d_c$	column inner diameter (cm)
$K_s$	Monod half-velocity constant ( $\text{g}\cdot\text{L}^{-1}$ )
$k_i$	film mass transfer coefficient of component $i$ ( $\text{cm}\cdot\text{s}^{-1}$ )
$k_s$	maximum specific substrate utilization rate averaged over the particle volume ( $\text{s}^{-1}$ )
$L$	column length (cm)
$Pe_{Li}$	Peclet number of axial dispersion for component $i$
$R$	radial coordinate for a particle in cylindrical coordinate system (cm)
$R_{ai}$	rate of addition of component $i$ per unit particle volume including macropores and particle skeleton ( $\text{g}\cdot\text{L}^{-1}\cdot\text{s}^{-1}$ )
$R_{a1}$	opposite of rate of depletion of substrate ( $\text{g}\cdot\text{L}^{-1}\cdot\text{s}^{-1}$ )
$R_{a2}$	rate of formation of product ( $\text{g}\cdot\text{L}^{-1}\cdot\text{s}^{-1}$ )
$r_{ai}$	$= R_{ai} L / (v C_{0i})$
$r$	$= R / R_p$
$R_p$	particle radius (cm)

$S$	substrate concentration ( $\text{g}\cdot\text{L}^{-1}$ )
$t$	dimensional time ( $t = 0$ is the moment a sample enters a column) (s)
$v$	interstitial velocity ( $\text{cm}\cdot\text{s}^{-1}$ )
$X$	immobilized cell mass concentration per unit particle volume including pores ( $\text{g dry cells}\cdot\text{L}^{-1}$ )
$X_0$	initial $X$ value at time zero ( $\text{g dry cells}\cdot\text{L}^{-1}$ )
$Y_{P/S}$	yield coefficient of product over substrate (g product/g substrate)
$y$	any real number
$Z$	column axial coordinate in cylindrical coordinate system (cm)
$z$	$= Z/L$

#### Greek Letters

$\epsilon_b$	bed void volume fraction
$\epsilon_p$	particle porosity
$\eta_i$	dimensionless group
$\lambda$	cell death rate ( $\text{s}^{-1}$ )
$\tau$	dimensionless time, $tv/L$
$\xi_i$	dimensionless constant

#### References and Notes

- (1) Shuler, M. L.; Kargi, F. *Bioprocess Engineering—Basic Concepts*; Prentice Hall: Upper Saddle River, 1992; pp 248–249.
- (2) Scott, C. D. Immobilized cells: a review of recent literature. *Enzyme Microb. Technol.* **1987**, *9*, 66–73.
- (3) Mosbach, K. *Immobilized Enzymes and Cells. Part B*; Academic Press: Orlando, 1987.
- (4) Park, J. K.; Chang, H. N. Microencapsulation of microbial cells. *Biotechnol. Adv.* **2000**, *18*, 303–319.
- (5) Lozinsky, V. I.; Galaev, I.; Yu, Plieva, F. M.; Savina, I. N.; Jungvid, H.; Mattiasson, B. Polymeric cryogels as promising materials of biotechnological interest. *Trends Biotechnol.* **2003**, *21*, 445–451.
- (6) Seki, M.; Furusaki, S. An immobilized cell system for taxol production. *Chemtech* **1996**, *26*, 41–45.
- (7) Benthack, C.; Srinivasan, B.; Bonvin, D. An optimal operating strategy for fixed-bed bioreactors used in wastewater treatment. *Biotechnol. Bioeng.* **2001**, *72*(1), 34–40.
- (8) Langley, W. G.; Wu, J. S.; Chao, A. C. Reaction kinetics of immobilized-cell denitrification. I: Background and model development. *J. Environ. Eng.* **2001**, *127*(8), 682–688.
- (9) Chen, K.-C.; Chen, C.-Y.; Peng, J.-W.; Houn, J.-Y. Real-time control of an immobilized-cell reactor for wastewater treatment using ORP. *Water Res.* **2002**, *36*, 230–238.
- (10) Cohen, Y. Biofiltration—the treatment of fluids by microorganisms immobilized into the filter bedding material: a review. *Bioresour. Technol.* **2001**, *77* 257–274.
- (11) Martin, M.; Mengs, G. Propachlor removal by *Pseudomonas* strain GCH1 in an immobilized-cell system. *Appl. Environ. Microbiol.* **2000**, *66*(3), 1190–1194.
- (12) Freeman, A.; Lilly, M. D. Effect of processing parameters on the feasibility and operational stability of immobilized viable microbial cells. *Enzyme Microb. Technol.* **1998**, *23*, 335–345.
- (13) Kim, C. J.; Chang, Y. K.; Chun, G.-T. Continuous culture of immobilized *Streptomyces* cells for kasugamycin production. *Biotechnol. Prog.* **2001**, *17*, 453–61.
- (14) Manohar, S.; Karegoudar, T. B.; Kim, C. K. Enhanced degradation of naphthalene by immobilization of *Pseudomonas* sp. strain NGK1 in polyurethane foam. *Appl. Microbiol. Biotechnol.* **2001**, *55*, 311–16.
- (15) Tanaka, A.; Tosa, A.; Kobayashi, T. *Industrial Application of Immobilized Biocatalysts*; Dekker: New York, 1993.
- (16) Riley, M. R.; Muzzio, F. J.; Reyes, S. C. Calculation of effective diffusivities and reactivities in immobilized cell systems using finite difference methods. *Comput. Chem. Eng.* **1998**, *22*, 525–534.
- (17) Galban, C. J.; Locke, B. R. Analysis of cell growth kinetics and substrate diffusion in a polymer scaffold. *Biotechnol. Bioeng.* **1999**, *65*(2), 121–132.
- (18) Gonzalez-Gil, G.; Seghezze, L.; Lettinga, G.; Kleerebezem, R. Kinetics and mass-transfer phenomena in anaerobic granular sludge. *Biotechnol. Bioeng.* **2001**, *73*(2), 126–134.
- (19) Wu, J. S.; Langley, W. G.; Chao, A. C. Reaction kinetics of immobilized-cell denitrification. II: Experimental study. *J. Environ. Eng.* **2001**, *127*(8), 689–697.
- (20) Nath, S.; Chand, S. Mass transfer and biochemical reaction in immobilized cell packed bed reactors: correlation of experiment with theory. *J. Chem. Technol. Biotechnol.* **1996**, *66*, 286–292.
- (21) Zheng, Y.; Gu, Y. Analytical solution to a model for the startup period for fixed-bed reactors. *Chem. Eng. Sci.* **1996**, *51*(15), 3773–3779.
- (22) Gu, T. *Mathematical Modeling and Scale-Up of Liquid Chromatography*; Springer: Berlin-New York, 1995.
- (23) Bailey, J. E.; Ollis, D. F. *Biochemical Engineering Fundamentals*, 2nd ed.; McGraw-Hill: New York, 1996; p 421.
- (24) Brown, P. N.; Byrne, G. D.; Hindmarsh, A. C. VODE: A variable coefficient ODE solver. *SIAM J. Sci. Stat. Comput.* **1989**, *10*, 1038–1051.
- (25) Weber, S. G.; Carr, P. W. The theory of the dynamics of liquid chromatography. In *High Performance Liquid Chromatography*; Brown, P. R., Hartwick, R. A., Eds.; Wiley: New York, 1989; pp 1–115.
- (26) Gu, T.; Tsai, G.-J.; Tsao, G. T. A theoretical study of multicomponent radial flow chromatography. *Chem. Eng. Sci.* **1991**, *46*(5/6), 1279–1288.
- (27) Pfeffer, R.; Happel, J. An analytical study of heat and mass transfer in multiparticle systems at low Reynolds numbers. *AIChE J.* **1964**, *10*, 605–611.

Accepted for publication July 30, 2004.

BP049776K